Geophysical Research Letters

RESEARCH LETTER
10.1029/2023GL105323

Impacts of Climate Change on Coastal Hydrodynamics Around a Headland and Potential Headland Sediment Bypassing

Danghan Xie[1], Zoe Hughes[1], Duncan FitzGerald[1], Silke Tas[1,2], Tansir Zaman Asik[1], and Sergio Fagherazzi[1]

[1]Department of Earth and Environment, Boston University, Boston, MA, USA, [2]Hydrology and Environmental Hydraulics Group, Wageningen University and Research, Wageningen, The Netherlands

Key Points:

- The formation of circulation cells and wave energy convergence around headlands during storms reduce bottom shear stress at the beach
- Sea-level rise increases wave heights, currents, and bed shear stress in the nearshore because of landward shifting of the circulation cells
- Higher storm waves expand the surf zone, shift circulation cells seaward, and enhance potential headland sediment bypassing

Supporting Information:

Supporting Information may be found in the online version of this article.

Correspondence to:

D. Xie,
danghan@bu.edu

Citation:

Xie, D., Hughes, Z., FitzGerald, D., Tas, S., Asik, T. Z., & Fagherazzi, S. (2024). Impacts of climate change on coastal hydrodynamics around a headland and potential headland sediment bypassing. *Geophysical Research Letters*, *51*, e2023GL105323. https://doi.org/10.1029/2023GL105323

Received 6 JULY 2023
Accepted 27 JAN 2024

Abstract Shorelines face growing threats due to climate change and diminishing sand supply. Coastal headlands, common rocky features along coastlines, are crucial in shaping hydrodynamics and sediment transport. Yet, the influence of future climate conditions, including sea-level rise (SLR) and intensified storm energy on complex shorelines with headlands has remained relatively unexplored. In this study, we model changes in hydrodynamics and headland bypassing under different SLR and higher storm wave scenarios. Our findings reveal the formation of circulation cells on both sides of a headland, where wave energy converges around the headland zone. Future climate conditions result in larger storm waves on the beach. However, SLR enhances nearshore currents through a landward shifting of the circulation cells, while higher storm waves intensify offshore flow currents due to the seaward movement of the cells. This effect, in turn, increases the potential for headland sediment bypassing.

Plain Language Summary Coastal headlands, prominent rocky features along open coastlines, play a crucial role in protecting nearby beaches from strong waves and erosion. They also affect how sand is exchanged between different beaches. We use a model to explore how future climate conditions including sea-level rise (SLR) and larger storm waves influence coastal waves, littoral currents, and the transport of sand around headlands. Our findings reveal that headlands converge wave energy forming circulation flow cells. SLR results in stronger nearshore currents, driven by the landward movement of the rotating flow cells. In contrast, larger storm waves can move the rotating flow cells seaward, thereby increasing offshore current strength and the potential for sand transport around the headland. Understanding how coastal waves, flow and sediment transport change under future climate conditions will help determine coastal resilience.

1. Introduction

The coastal zone contains a variety of landforms that provide valuable ecosystem services and recreational areas for coastal communities. However, the stability of coastlines is of growing concern because of the increasing risks posed by climate change, including the accelerating rate of sea-level rise (SLR) and the increasing frequency and intensity of storms (Church & White, 2011; Hallegatte et al., 2013; Xie et al., 2020). The consequent enhanced hydrodynamic forces are expected to cause greater erosion, further degrading the shore (Ashton & Murray, 2006; Masselink et al., 2016; Stockdonf et al., 2002).

Coastlines rarely exhibit straight profiles; instead, they often display indentations accompanied by coastal headlands, such as bay-headland coasts or embayed coasts (Davis & FitzGerald, 2020; Slott et al., 2006; van Rijn, 2011). Headlands are a common coastal landform found along nearly 80% of the ice-free shorelines worldwide (Klein et al., 2020; Luijendijk et al., 2018; Nyberg & Howell, 2016). They typically consist of sedimentary rocks which are more resistant to erosion, allowing them to protrude further into the water as the adjacent beach recedes (Davis & FitzGerald, 2020; Limber & Murray, 2011; Ramesh et al., 2021).

Previous studies have identified the key characteristics of coastal headlands, including: (a) converging points for wave energy and currents; (b) obstruction of littoral drifts; (c) blockage of wave energy, creating sheltered areas along adjacent beaches; and (d) formation of circulation cells in nearby waters (Bastos et al., 2003; da Silva et al., 2021; Klein et al., 2020; McCarroll et al., 2019; van Rijn, 1998). These characteristics not only shape local geomorphology but also significantly impact sediment dynamics throughout the coastal system (George et al., 2022). For example, the concentration of hydrodynamic forces around headlands reduces longshore

currents, promoting local sedimentation (van Rijn, 2011). Additionally, sediment connectivity between adjacent embayments around a headland, accomplished through headland bypassing, strongly influences sediment availability and subsequent sedimentation patterns in the downdrift areas (Klein et al., 2020). However, the efficiency of headland bypassing varies with individual systems depending on wave incident angles, wave heights and shape of the headland (George et al., 2019). A noteworthy phenomenon that arises around headlands is the formation of circulation cells, resulting from the interactions among waves, currents, and coastal geomorphology. These circulation cells play a vital role in governing sediment transport processes as sediment is driven and redistributed by the circulation currents (George et al., 2019; Klein et al., 2020; McCarroll et al., 2018).

The dynamics of circulation cells and headland bypassing are significantly influenced by the interplay of tides and waves. Vieira da Silva et al. (2018) found that waves are the driving force producing circulation cells leading to headland bypassing, with tides playing a secondary role. This perspective is reinforced by other studies underlining the role that large waves have for the initiation of sediment bypassing (McCarroll et al., 2018; Thom et al., 2018). Tidal levels and tidal currents are also important. Research by Costa et al. (2019) suggests that tidal currents can complement and reinforce wave-driven sediment transport, thereby favoring sediment bypassing around the headland. Similar findings has been found by Valiente et al. (2019), who observed that heightened tidal levels intensify nearshore bed shear stress, augmenting headland bypassing. Despite these recent insights, the effect of climate change such as SLR and higher storm waves remains relatively unexplored (George et al., 2022; Klein et al., 2020). SLR has the potential to deepen shallow coastal areas and reduce wave attenuation, enabling greater penetration of wave energy closer to the shore (Siegle & Costa, 2017). On the other hand, larger wave energy intensifies wave heights and alter the wave breaking zone (Peregrine, 1983). Both aspects have implications for the hydrodynamics of headlands and, consequently, headland bypassing. Thus, there is a need for comprehensive research aimed at unraveling how climate change drivers may impact headlands, and by extension, the patterns of headland bypassing.

Here we investigate the impact of headlands on coastal hydrodynamics and potential headland bypassing, as well as assess how these impacts may change under rising sea level and increased storm magnitude conditions. Our study focuses on Western Buzzards Bay (Figure 1a), consisting of a major coastal headland separating two embayments (FitzGerald et al., 1987). We conduct numerical modeling to explore the impacts of coastal headlands on nearshore hydrodynamics and the effects of climate change on coastal vulnerability. This study improves our understanding of physical forces operating along indented shorelines under future climate conditions.

2. Materials and Methods

2.1. Study Area

Western Buzzards Bay, Massachusetts (USA), includes numerous tidal inlets and estuaries. The bay is characterized by indented shorelines separated by headlands and embayments (Figure 1b). The Gooseberry Island headland in this study is an offshore island attached to the shoreline by a natural tombolo and, more recently, by a manmade causeway similar to the study by Klein et al. (2020). The island shore is mantled by cobbles and boulders with a general elevation higher than 1 m, so that the island shoreline is relatively stable and unlikely to be flooded in a regime of a 1-m SLR (Figure S1 in Supporting Information S1). Where beaches do exist, they are primarily composed of fine sand and often armored by coarse sand and gravel layers (FitzGerald et al., 1992). The system is wave dominated and experiences a relatively small tidal range (~1.1 m), with a modest river discharge (~2 m^3/s) (Figure S2 in Supporting Information S1) (Bent, 1995; FitzGerald et al., 1987). Prevailing winds and waves originate from the southwest due to the sheltering effect of the Elizabeth Islands that extend southwestward from Cape Cod (Figure 1a; Figure S3 in Supporting Information S1). The area is commonly impacted by extratropical cyclones and infrequent hurricanes, both of which could generate over 5 m significant wave heights at a 21-m water depth (Figure 1c), driving sediment resuspension, shoreline retreat, and inlet breaching (FitzGerald et al., 2002).

2.2. General Description of Model Approach

Following previous studies of coastal circulation cells (McCarroll et al., 2018; Mulligan et al., 2008; van Rijn, 2011), the process-based model Delft3D was used to simulate coastal hydrodynamics, during varying storm conditions and different climate scenarios (Lesser et al., 2004). Delft3D-FLOW solves the depth-averaged shallow water equations to simulate water levels and current velocity (Lesser et al., 2004). Delft3D-WAVE

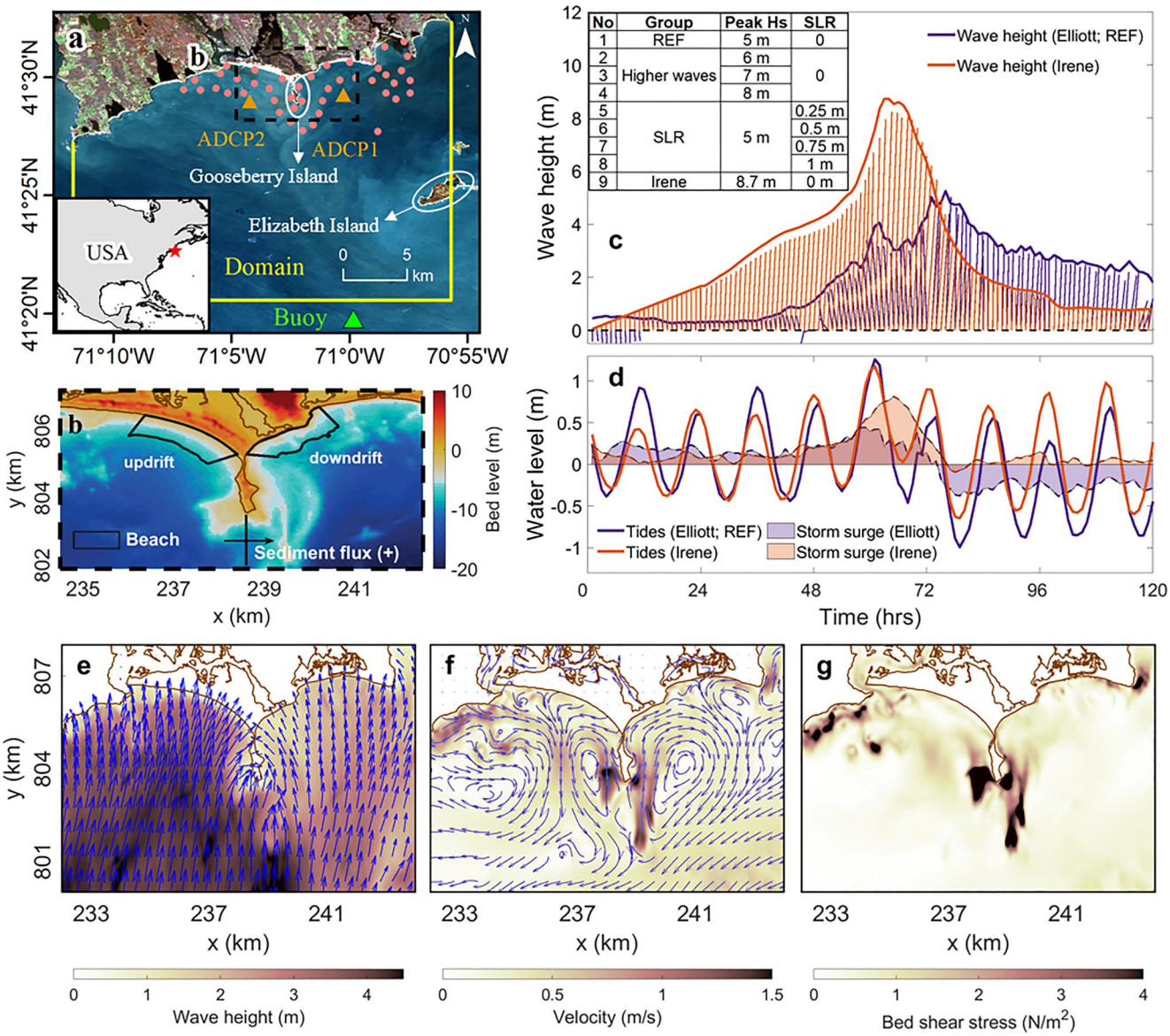

Figure 1. Model regions in the study area (Western Buzzards Bay, MA, USA), boundary conditions and key hydrodynamic parameters around the headland during the present-day storm conditions. (a) The Delft3D-FLOW and Delft3D-WAVE domains overlap in the region depicted by the yellow box. Black dashed box highlights the focus area of this research, consisting of two coastal cells separated by a headland. Red dots are validation points extracted from the North Atlantic Coast Comprehensive Study Coastal Hazards System (Cialone et al., 2015) (Text S1 in Supporting Information S1). Two Acoustic Doppler Current Profiler (ADCPs) are deployed updrift and downdrift of the headland, measuring water level and waves (e.g., significant wave height [Hs], peak wave period and wave direction); this data set is used to validate the model setup. Green triangle shows the location of an offshore buoy (Station No.: BUZM3 & 44085; 21-m water depth) recording hydrodynamic and meteorological data for model setup. (b) Topographic map of the focus area indicating both updrift and downdrift beaches (black outline). The offshore boundary of each region is based on the 8-m water line determined by the Depth of Closure (see Text S4 in Supporting Information S1) (Hallermeier, 1978; King et al., 2021; Valiente et al., 2019). (c) Wave height, and (d) water level signals at the domain boundary of two historical storms (Elliott and Irene). Lines in panel (c) point to the direction where the waves are propagating toward. In panel (c), scenarios with higher storm waves and sea-level rise (SLR) are presented, with Storm Elliott as the reference (REF). (e) Wave propagation map, (f) flow velocity field with the formation of circulation cells on both sides of the headland, and (g) bed shear stress. Panels (e)–(g) are based on the Elliott storm (2022) and serve as reference results in Figures 2 and 3.

simulates wave propagation and dissipation (whitecapping, bottom friction, and depth-induced breaking) as well as wave-current interactions, based on the third-generation spectral wave model Simulating WAves Nearshore (Booij et al., 1999). Delft3D-FLOW and Delft3D-WAVE were coupled in a two-way manner using overlapping grids (Figure 1a). This allows for the consideration of the impacts of flow on waves (via set-up, current refraction and enhanced bottom friction), as well as the effects of waves on currents (via forcing and enhanced bed shear

stress) (Deltares, 2014). Since the river discharge is small in our study site, vertical stratification of the water column is assumed to be negligible and is not included (Garrison, 2014).

Bottom shear stress are enhanced due to the non-linear interaction between the boundary layer at the bed associated with the waves and the current (Grant & Madsen, 1979). The enhancement of the bed shear stress (τ_m) is calculated using Soulsby et al. (1993) formula:

$$\tau_m = \tau_c \left[1 + 1.2 \left(\frac{\tau_w}{\tau_w + \tau_c} \right)^{3/2} \right] \quad (1)$$

where the bed shear stress driven by current alone (τ_c) is related to the Chézy friction value (C) and current velocity (u):

$$\tau_c = \frac{g \rho u^2}{C^2} \quad (2)$$

and τ_w is the wave-induced bed shear stress:

$$\tau_w = \frac{1}{2} \rho f_w u_{\text{orb}}^2 \quad (3)$$

where $g = 9.81$ m/s^2 is the gravitational acceleration and ρ is the density of water, set to 1,025 kg/m^3. Wave friction (f_w) is calculated in Delft3D-FLOW using Swart (1974) formula after the wave orbital velocity near the bottom (u_{orb}) is computed from Delft3D-WAVE. Other details on grid development, bathymetry sources, boundary conditions and model validation are provided in Supporting Information S1 (Texts S2 and S3 in Supporting Information S1).

2.3. Model Scenario Setups

Previous studies indicate that climate change is responsible for SLR and higher wave energy, which can intensify hydrodynamic forces around coastal areas (FitzGerald et al., 2020). To investigate these effects, we divided modeling simulations into three groups: present-day scenarios (the reference run with Storm Elliott), future climate change scenarios (derived from the reference run), and another real storm event (Hurricane Irene) (see table in Figure 1c). In the climate change scenarios, we simulated different peak wave heights and various SLR magnitudes. The storm wave heights were selected using the annual wave exceedance probability for wave heights from the North Atlantic Coast Comprehensive Study (NACCS) (Figure S4a in Supporting Information S1) (Cialone et al., 2015). The SLR scenarios for the model were based on the NOAA technical report for the United States coast (Figure S4b in Supporting Information S1) (Sweet et al., 2022).

We investigated the effects of different values of SLR by setting up four additional runs, where the mean water level during the Storm Elliott was increased by 0.25, 0.5, 0.75, and 1 m. These values represent future projections of mean water levels along the US coastline. Sea level will increase by 0.3 m in 2050 and 1 m by 2090 based on the IPCC Intermediate climate scenario, which anticipates global mean sea level reaching 1 m by 2100 (Figure S4b in Supporting Information S1).

The peak wave height of Storm Elliott at the buoy is around 5 m, which corresponds to a storm with yearly frequency (Figure S4a in Supporting Information S1). To assess the effects of higher storm waves on the system resulting from climate change, we conducted additional simulations using peak storm wave heights of 6, 7, and 8 m at the buoy, representing return periods of approximately 2, 3, and 5 years, respectively (Figure S4a in Supporting Information S1).

3. Results

3.1. Effects of Sea-Level Rise and Higher Storm Waves on Coastal Circulation Cells

We show that coastal headlands concentrate wave energy and induce two circulation cells at the two sides. The cells lead to higher hydrodynamic forces around the headland than adjacent beaches during storms (Figures 1e–

1g). For the present-day scenario, the headland creates a shadow zone downdrift when waves come from the south to southwest, causing higher wave height in the updrift beach (Figure 1e). In addition, the headland produces wave refraction that redistributes wave energy along the adjacent nearshore (Figure 1e). Circulation cells caused by wave breaking along both sides of the headland diverge the flow current from the headland thereby lessening current magnitude along the bordering embayments (Figure 1f). The presence of circulation cells and convergence of wave energy create higher bed shear stress around the headland than along the adjacent beaches (Figure 1g).

Both SLR and the presence of higher storm waves increase nearshore wave heights, yet the two climate change scenarios display distinct impacts on coastal currents and bottom shear stress, as depicted in Figures 2 and 3.

Higher water levels during storms extend the propagation of waves closer to the shoreline, resulting in higher wave heights along both updrift and downdrift beaches and in proximity to the headland (Figure 2a). SLR causes the onshore migration of the circulation cells. This migration intensifies currents in shallow areas, and augments bed shear stress along the beach and in the vicinity of the headland (Figures 2b and 2c). Conversely, scenarios featuring higher storm waves produce an increase in wave heights along the beach while maintaining relatively consistent conditions around the headland (Figure 3a). However, these scenarios present a seaward migration of circulation cells, causing a reduction in flow strength and bed shear stress near the shoreline and along both sides of the headland, accompanied by an increase in flow strength and bed shear stress around the seaward side of the headland (Figures 3b and 3c). In the event of both high storm surge and storm waves, as exemplified by the Irene scenario, the beach and the headland are exposed to higher waves, leading to the expansion of the circulation cells, especially on the downdrift side of the headland (Figures 3a and 3b). This expansion contributed to increased current velocity and stronger bed shear stress in the downdrift beach, contrasting with the relatively minimal changes observed in flow strength and bed shear stress in the updrift beach (Figures 3b and 3c).

3.2. How Sea-Level Rise and Higher Storm Waves Affect Potential Headland Bypassing

To assess sediment bypassing around the headland, we consider a hypothetical system with a seabed composed entirely of sand. We calculate the potential sediment flux across a transect in front of the headland (see Figure 1b). This flux is primarily influenced by storm wave height, as shown in Figure 4.

In the present-day scenario, the sediment flux is nearly negligible (gray violin in Figure 4), and SLR has limited impact on it (blue violins in Figure 4a). In contrast, larger storm waves significantly enhance the potential sediment flux (green violins in Figure 4b). In addition, our results show that a storm surge has a significant impact on headland passing. The storm surge from Hurricane Irene is nearly double that of Storm Elliott (Figure 1d). Compared to an 8-m wave height scenario, a similar wave height scenario with a larger storm surge (i.e., hurricane Irene) could almost triple the potential sediment flux (Figure 4b).

4. Discussion and Conclusions

The role of headlands in the coastal system has been a topic of interest for decades, yet the effects of future climate conditions on coastal hydrodynamics around headlands and on the potential headland bypassing remain relatively unexplored. Our modeling findings indicate that future climate conditions are likely to result in increased wave heights nearshore. Nevertheless, our findings reveal that distinct patterns of flow and hydrodynamic forces around the headland can emerge under different climate scenarios, such as SLR and higher storm waves. These differing behaviors can lead to contrasting responses in terms of headland bypassing.

The presence of a coastal headland is known to concentrate waves, resulting in decreased wave energy in adjacent beach regions (Goodwin et al., 2013; McCarroll et al., 2020; Wishaw et al., 2020). The shallow areas surrounding these headlands not only mitigate wave heights but also intensify flow currents due to wave breaking, creating additional forces on currents (Dobbelaere et al., 2022; McCarroll et al., 2020). These effects are consistent with our simulations, which reveal the development of circulation cells around the headland, characterized by accelerated flow currents along the shallow zones (Figure 1f). This phenomenon aligns with previous studies (Valiente et al., 2019) and is essential in directing offshore flows and redistributing sediment within the coastal system (George et al., 2019; Mouragues et al., 2020). Our simulation suggests that bed shear stress is strongly related to the circulation cells (Figure 1g), potentially controlling sediment transport patterns, coastal erosion, and shoreline stability (Marchesiello et al., 2019).

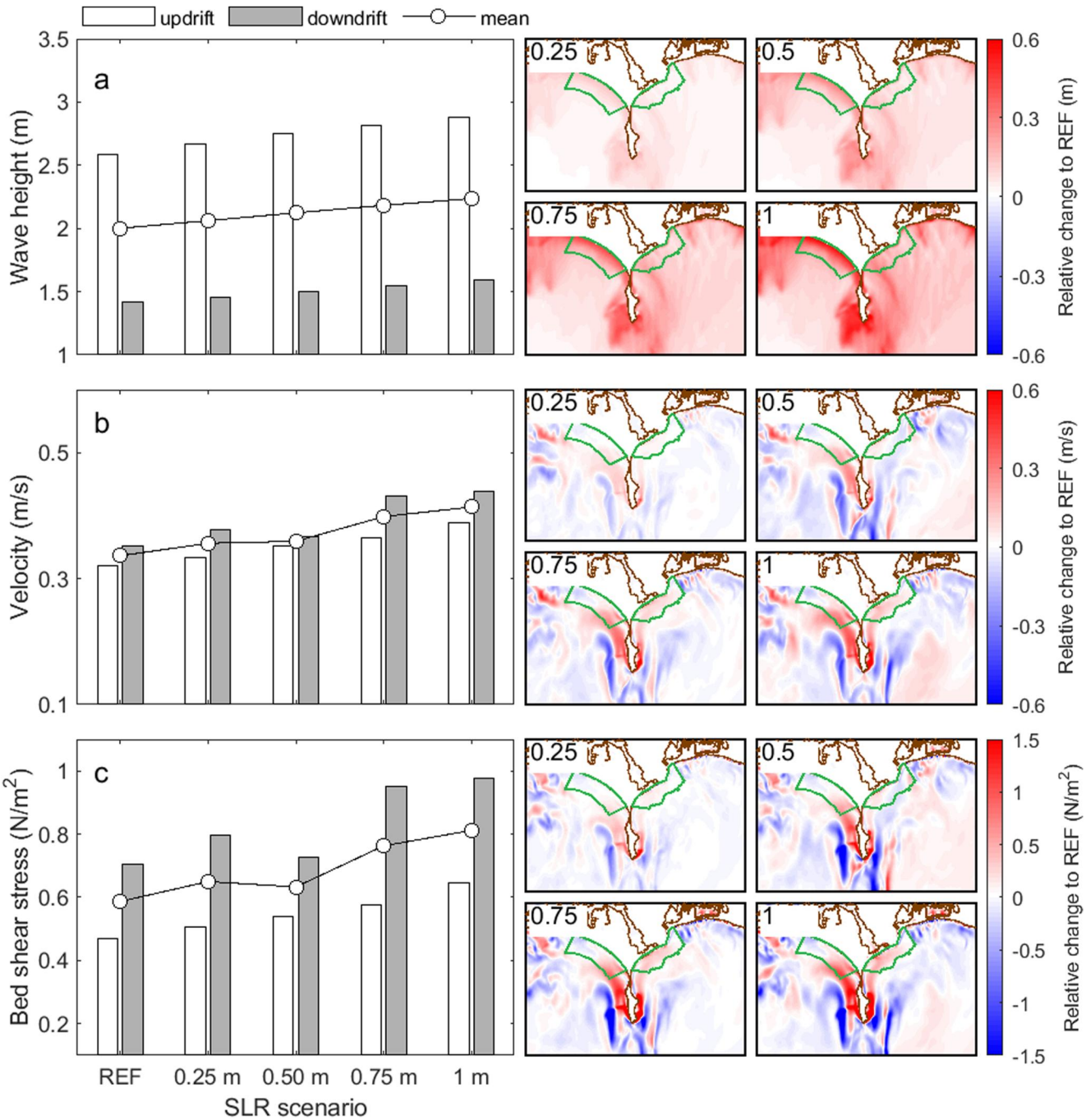

Figure 2. Changes in wave height, velocity, and bed shear stress under different sea-level rise (SLR) scenarios. The bar graphs in the left panel are based on the median values of these hydrodynamic parameters in the updrift and downdrift beach regions, respectively. The mean of two bar values is represented by circles on the graph. The spatial distribution of the relative changes in these three hydrodynamic parameters is presented in the right panel. These relative changes are based on the reference results from Figures 1e–1g.

We have also examined how different climate scenarios impact the hydrodynamic environment around the headland. Our findings reveal opposing behaviors of circulation cells in response to SLR and higher storm wave scenarios, affecting both velocity and bottom shear stress on the beach (Figures 2 and 3) and potentially influencing headland bypassing (Figure 4). In the SLR scenarios, higher water levels allow waves to propagate farther into both beach and headland areas (Figure 2a). This is due to the primary wave-breaking zone moving closer to the shore simultaneously with SLR, leading to higher flow velocity and bed shear stress along the beach

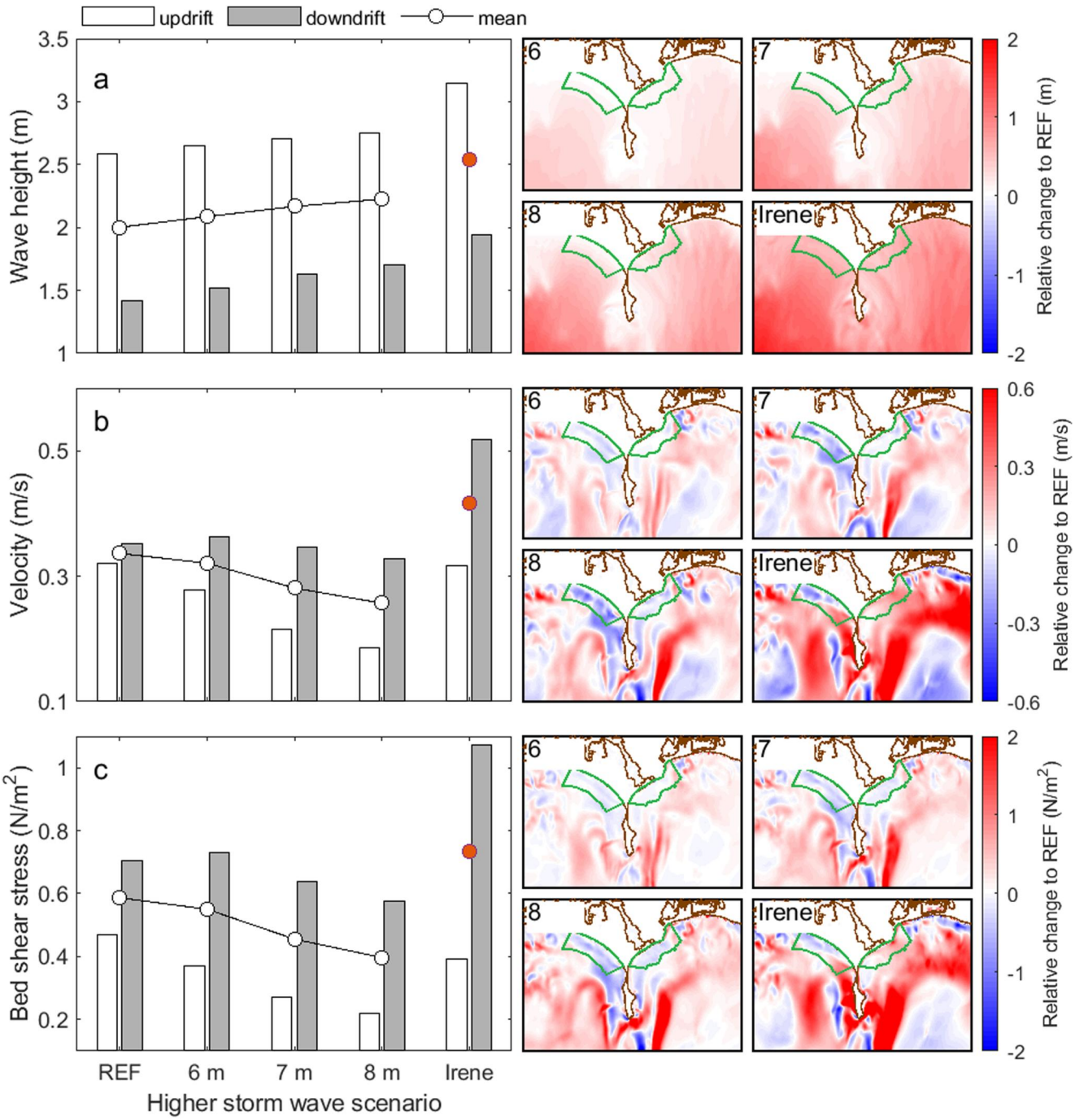

Figure 3. Changes in wave height, velocity, and bed shear stress under different scenarios of storm waves. The bar graphs in the left panel are based on the median values of these hydrodynamic parameters from the updrift beach region and the downdrift beach region, respectively. The mean of two bar values is represented by circles on the graph. The spatial distribution of the relative changes in these three hydrodynamic parameters is presented in the right panel. These relative changes are based on the reference results from Figures 1e–1g. Hydrodynamic parameters of Hurricane Irene are provided for a comparison.

(Figures 2b and 2c). In contrast, increased wave energy predominantly elevates wave height offshore of the beach rather than around the headland (Figures 2a and 3a), reducing both velocity and bed shear stress along the beach (Figures 3b and 3c). In these scenarios, the wave-breaking zone expands with intensified energy dissipation occurring at the edge of shallow areas, around the 10-m isobath (Figure S5 in Supporting Information S1). As a result, these distinct wave energy dissipation patterns intensify nearshore circulation cells in the SLR scenarios versus offshore circulation currents in higher storm wave scenarios (Figure 2b vs. Figure 3b). These findings align

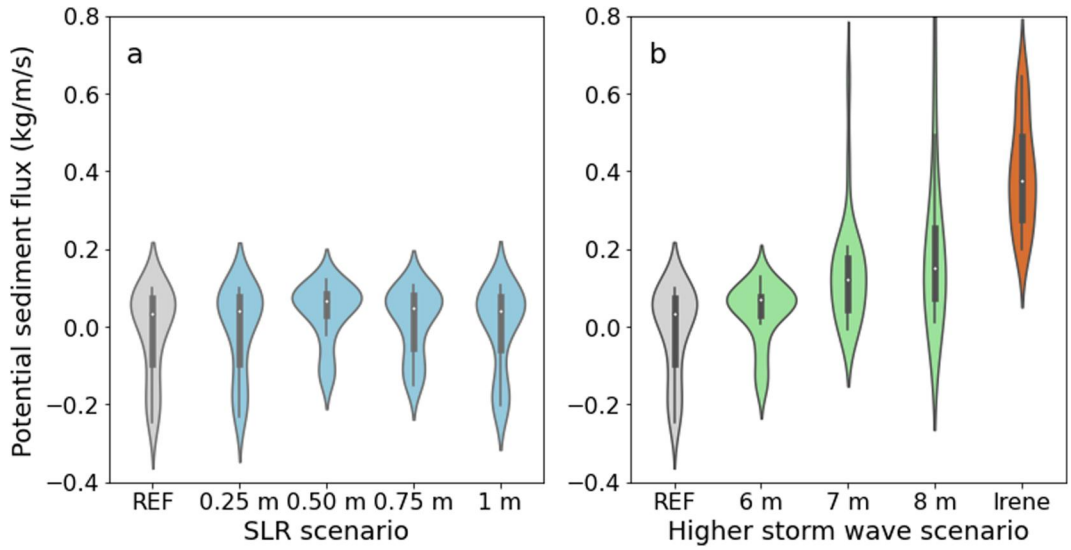

Figure 4. Potential sediment flux along the transect in front of the headland under different sea-level rise (SLR) scenarios (a) and higher storm wave scenarios (b). A positive sediment flux indicates sediment movement from the updrift coastal area to the downdrift area. Violin thickness corresponds to probability density. Endpoints of the violin depict minimum and maximum values. The box plot inside each violin covers the first to third quartiles, with a square representing the median value.

with similar studies by Mouragues et al. (2020), which also highlight that increasing wave height expands the surf zone area and causes the circulation cells to move to deeper waters. Our additional analysis further suggests that the increase in velocity or bed shear stress due to SLR is balanced by increasing wave height, leading to minimal changes in these two variables under certain combinations (Figure S6 in Supporting Information S1). Hence, the combinations of SLR and wave height are of critical importance in determining hydrodynamic changes along the beach in the future.

Potential headland bypassing is examined by evaluating the sediment flux along a transect near the headland (Figure 4). Our simulations indicate that headland bypassing is primarily facilitated by higher storm waves rather than SLR. The reason is that higher waves expand the surf zone, a phenomenon known to enhance headland bypassing, as demonstrated in both our Figure S5 in Supporting Information S1 and previous research (King et al., 2021). Nonetheless, the extent of headland bypassing is also controlled by factors such as spatial sediment coverage and sediment grain size (George et al., 2019; King et al., 2021; Klein et al., 2020). Given that the primary sediment composition around the headland is sedimentary rocks, our domain of only sand might overestimate the amount of headland bypassing (Davis & FitzGerald, 2020; Limber & Murray, 2011; Ramesh et al., 2021). Wave energy is usually believed to be the primary driver of headland bypassing, with tides playing a secondary role (King et al., 2021). Our study further suggests an additional factor that can enhance headland bypassing: storm surges. For example, in scenarios involving a storm surge twice as large as the reference scenario, we observe a threefold increase in headland bypassing, as illustrated in Figure 4b (8-m higher wave scenario vs. Hurricane Irene).

Recent studies have explored the impact of future climate change on coastal processes (Toimil et al., 2020). Coastal headlands, a common feature in shoreline systems worldwide, play a unique role in shaping these processes (Klein et al., 2020; Luijendijk et al., 2018; Nyberg & Howell, 2016). Climate-driven variations in hydrodynamics and sediment availability at the shore are crucial for coastal morphological development and will have dramatic ecological and economic implications (Xie et al., 2022). Our study highlights the complexities of physical forces operating along indented shorelines and different roles played by varying climate conditions in altering wave energy, circulation cells and the potential bypassing around headlands.

Data Availability Statement

The wind and wave data are collected from an offshore buoy station (Station No.: BUZM3 & 44085) maintained by National Data Buoy Center (NDBC, 2023). Historical tidal level is retrieved from Newport tidal gauge (Station

No.: 8452660) operated by National Oceanic and Atmospheric Administration (NOAA, 2023). Annual river discharge is measured at the Paskamanset River near South Dartmouth, Massachusetts, USA (Station No. 01105933, Location: 41°35′07″N, 70°59′27″W) managed by United States Geological Survey (USGS, 2023). Delft3D is an open-source code available online (Deltares, 2014). The model setup for a reference scenario and the hydrodynamic data utilized in this research are available in the Zenodo repository with open access under the MIT license (Xie, 2023). Model validation data includes the field observation (Acoustic Doppler Current Profiler) and regional modeling data set by NACCS Coastal Hazards System (Cialone et al., 2015).

Acknowledgments
Funding for this project was gratefully received from the Buzzards Bay Coalition through a grant from The Rathmann Family Foundation.

References

Ashton, A. D., & Murray, A. B. (2006). High-angle wave instability and emergent shoreline shapes: 1. Modeling of sand waves, flying spits, and capes. *Journal of Geophysical Research*, *111*(F4), F04011. https://doi.org/10.1029/2005jf000422

Bastos, A., Collins, M., & Kenyon, N. (2003). Water and sediment movement around a coastal headland: Portland Bill, Southern UK. *Ocean Dynamics*, *53*(3), 309–321. https://doi.org/10.1007/s10236-003-0031-1

Bent, G. C. (1995). *Streamflow, ground-water recharge and discharge, and characteristics of surficial deposits in Buzzards Bay Basin, Southeastern Massachusetts*. US Geological Survey.

Booij, N., Ris, R. C., & Holthuijsen, L. H. (1999). A third-generation wave model for coastal regions: 1. Model description and validation. *Journal of Geophysical Research*, *104*(C4), 7649–7666. https://doi.org/10.1029/98jc02622

Church, J. A., & White, N. J. (2011). Sea-level rise from the late 19th to the early 21st century. *Surveys in Geophysics*, *32*(4–5), 585–602. https://doi.org/10.1007/s10712-011-9119-1

Cialone, M. A., Massey, T. C., Anderson, M. E., Grzegorzewski, A. S., Jensen, R. E., Cialone, A., et al. (2015). North Atlantic Coast Comprehensive Study (NACCS) coastal storm model simulations: Waves and water levels. Retrieved from https://chs.erdc.dren.mil/Home. [Coastal Hazards System].

Costa, W. L. L., Silveira, L. F., & Klein, A. H. F. (2019). Influence of wave climate and tidal regime on headland bypassing - Study case: Northern São Francisco do Sul Island, SC, Brazil. In *Coastal sediments* (pp. 488–501).

da Silva, A. P., da Silva, G. V., Strauss, D., Murray, T., Woortmann, L. G., Taber, J., et al. (2021). Headland bypassing timescales: Processes and driving forces. *Science of the Total Environment*, *793*, 148591. https://doi.org/10.1016/j.scitotenv.2021.148591

Davis, R. A. J., & FitzGerald, D. M. (2020). *Beaches and coasts* (2nd ed.). John Wiley & Sons.

Deltares. (2014). Simulation of multi-dimensional hydrodynamic flows and transport phenomena, including sediments - User manual (Version: 3.15.34158) [Delft3D Software]. Deltares. Retrieved from https://oss.deltares.nl/

Dobbelaere, T., Curcic, M., Le Hénaff, M., & Hanert, E. (2022). Impacts of Hurricane Irma (2017) on wave-induced ocean transport processes. *Ocean Modelling*, *171*, 101947. https://doi.org/10.1016/j.ocemod.2022.101947

FitzGerald, D. M., Baldwin, C. T., Ibrahim, N. A., & Humphries, S. M. (1992). Sedimentologic and morphologic evolution of a beach ridge barrier along an indented coast: Buzzards Bay, Massachusetts.

FitzGerald, D. M., Baldwin, C. T., Ibrahim, N. A., & Sands, D. R. (1987). Development of the northwestern Buzzards Bay shoreline, Massachusetts. In *Glaciated coasts* (pp. 327–357). Academic Press, Inc. 18 fig, 38 ref.

FitzGerald, D. M., Buynevich, I. V., Davis, R. A., & Fenster, M. S. (2002). New England tidal inlets with special reference to riverine-associated inlet systems. *Geomorphology*, *48*(1), 179–208. https://doi.org/10.1016/s0169-555x(02)00181-2

FitzGerald, D. M., Hughes, Z. J., Georgiou, I. Y., Black, S., & Novak, A. (2020). Enhanced, Climate-driven sedimentation on salt marshes. *Geophysical Research Letters*, *47*(10), e2019GL086737. https://doi.org/10.1029/2019gl086737

Garrison, T. S. (2014). *Essentials of oceanography*. Cengage Learning.

George, D. A., Castelle, B., & Mulligan, R. P. (2022). Crossing the boundaries: How key advancements in understanding of headland sediment bypassing improves definition of littoral cells. *Journal of Geophysical Research: Oceans*, *127*(8), e2021JC018269. https://doi.org/10.1029/2021jc018269

George, D. A., Largier, J. L., Pasternack, G. B., Barnard, P. L., Storlazzi, C. D., & Erikson, L. H. (2019). Modeling sediment bypassing around idealized rocky headlands. *Journal of Marine Science and Engineering*, *7*(2), 40. https://doi.org/10.3390/jmse7020040

Goodwin, I. D., Freeman, R., & Blackmore, K. (2013). An insight into headland sand bypassing and wave climate variability from shoreface bathymetric change at Byron Bay, New South Wales, Australia. *Marine Geology*, *341*, 29–45. https://doi.org/10.1016/j.margeo.2013.05.005

Grant, W. D., & Madsen, O. S. (1979). Combined wave and current interaction with a rough bottom. *Journal of Geophysical Research*, *84*(C4), 1797–1808. https://doi.org/10.1029/jc084ic04p01797

Hallegatte, S., Green, C., Nicholls, R. J., & Corfee-Morlot, J. (2013). Future flood losses in major coastal cities. *Nature Climate Change*, *3*(9), 802–806. https://doi.org/10.1038/nclimate1979

Hallermeier, R. J. (1978). Uses for a calculated limit depth to beach erosion. In *Coastal engineering 1978* (pp. 1493–1512).

King, E. V., Conley, D. C., Masselink, G., Leonardi, N., McCarroll, R. J., Scott, T., & Valiente, N. G. (2021). Wave, tide and topographical controls on headland sand bypassing. *Journal of Geophysical Research: Oceans*, *126*(8), e2020JC017053. https://doi.org/10.1029/2020jc017053

Klein, A. H., da Silva, G. V., Taborda, R., da Silva, A. P., & Short, A. D. (2020). Headland bypassing and overpassing: Form, processes and applications. In *Sandy beach morphodynamics* (pp. 557–591).

Lesser, G. R., Roelvink, J. A., van Kester, J. A. T. M., & Stelling, G. S. (2004). Development and validation of a three-dimensional morphological model. *Coastal Engineering*, *51*(8–9), 883–915. https://doi.org/10.1016/j.coastaleng.2004.07.014

Limber, P. W., & Murray, A. B. (2011). Beach and sea-cliff dynamics as a driver of long-term rocky coastline evolution and stability. *Geology*, *39*(12), 1147–1150. https://doi.org/10.1130/g32315.1

Luijendijk, A., Hagenaars, G., Ranasinghe, R., Baart, F., Donchyts, G., & Aarninkhof, S. (2018). The state of the world's beaches. *Scientific Reports*, *8*(1), 1–11. https://doi.org/10.1038/s41598-018-24630-6

Marchesiello, P., Nguyen, N. M., Gratiot, N., Loisel, H., Anthony, E. J., San Dinh, C., et al. (2019). Erosion of the coastal Mekong delta: Assessing natural against man induced processes. *Continental Shelf Research*, *181*, 72–89. https://doi.org/10.1016/j.csr.2019.05.004

Masselink, G., Scott, T., Poate, T., Russell, P., Davidson, M., & Conley, D. (2016). The extreme 2013/2014 winter storms: Hydrodynamic forcing and coastal response along the southwest coast of England. *Earth Surface Processes and Landforms*, *41*(3), 378–391. https://doi.org/10.1002/esp.3836

McCarroll, R. J., Masselink, G., Valiente, N. G., Scott, T., King, E. V., & Conley, D. (2018). Wave and tidal controls on embayment circulation and headland bypassing for an exposed, macrotidal site. *Journal of Marine Science and Engineering*, *6*(3), 94. https://doi.org/10.3390/jmse6030094

McCarroll, R. J., Masselink, G., Valiente, N. G., Wiggins, M., Scott, T., Conley, D. C., & King, E. V. (2020). Impact of a headland-associated sandbank on shoreline dynamics. *Geomorphology*, *355*, 107065. https://doi.org/10.1016/j.geomorph.2020.107065

McCarroll, R. J., Masselink, G., Wiggins, M., Scott, T., Billson, O., Conley, D., & Valiente, N. (2019). High-efficiency gravel longshore sediment transport and headland bypassing over an extreme wave event. *Earth Surface Processes and Landforms*, *44*(13), 2720–2727. https://doi.org/10.1002/esp.4692

Mouragues, A., Bonneton, P., Castelle, B., Marieu, V., Jak McCarroll, R., Rodriguez-Padilla, I., et al. (2020). High-energy surf zone currents and headland rips at a geologically constrained mesotidal beach. *Journal of Geophysical Research: Oceans*, *125*(10), e2020JC016259. https://doi.org/10.1029/2020jc016259

Mulligan, R. P., Hay, A. E., & Bowen, A. J. (2008). Wave-driven circulation in a coastal bay during the landfall of a hurricane. *Journal of Geophysical Research*, *113*, C05026. https://doi.org/10.1029/2007jc004500

NDBC. (2023). Wind and wave data collected from National Data Buoy Center (Station No.: BUZM3 & 44085) [Dataset]. NDBC. Retrieved from https://www.ndbc.noaa.gov/

NOAA. (2023). Historical tidal level data retrieved from Newport tidal gauge under National Oceanic and Atmospheric Administration (Station No.:8452660) [Dataset]. NOAA. Retrieved from https://tidesandcurrents.noaa.gov/

Nyberg, B., & Howell, J. A. (2016). Global distribution of modern shallow marine shorelines. Implications for exploration and reservoir analogue studies. *Marine and Petroleum Geology*, *71*, 83–104. https://doi.org/10.1016/j.marpetgeo.2015.11.025

Peregrine, D. H. (1983). Breaking waves on beaches. *Annual Review of Fluid Mechanics*, *15*(1), 149–178. https://doi.org/10.1146/annurev.fl.15.010183.001053

Ramesh, R., Purvaja, R., Rajakumari, S., Suganya, G. M. D., Sarunjith, K. J., & Vel, A. S. (2021). Sediment cells and their dynamics along the coasts of India – A review. *Journal of Coastal Conservation*, *25*(2), 31. https://doi.org/10.1007/s11852-021-00799-3

Siegle, E., & Costa, M. B. (2017). Nearshore wave power increase on reef-shaped coasts due to sea-level rise. *Earth's Future*, *5*(10), 1054–1065. https://doi.org/10.1002/2017ef000624

Slott, J. M., Murray, A. B., Ashton, A. D., & Crowley, T. J. (2006). Coastline responses to changing storm patterns. *Geophysical Research Letters*, *33*, L18404. https://doi.org/10.1029/2006gl027445

Soulsby, R. L., Hamm, L., Klopman, G., Myrhaug, D., Simons, R. R., & Thomas, G. P. (1993). Wave-current interaction within and outside the bottom boundary layer. *Coastal Engineering*, *21*(1), 41–69. https://doi.org/10.1016/0378-3839(93)90045-a

Stockdonf, H. F., Sallenger, A. H., Jr., List, J. H., & Holman, R. A. (2002). Estimation of shoreline position and change using airborne topographic lidar data. *Journal of Coastal Research*, 502–513.

Swart, D. H. (1974). Offshore sediment transport and equilibrium beach profiles.

Sweet, W. V., Hamlington, B. D., Kopp, R. E., Weaver, C. P., Barnard, P. L., Bekaert, D., et al. (2022). *Global and regional sea level rise scenarios for the United States: Updated mean projections and extreme water level probabilities along US coastlines*. National Oceanic and Atmospheric Administration.

Thom, B. G., Eliot, I., Eliot, M., Harvey, N., Rissik, D., Sharples, C., et al. (2018). National sediment compartment framework for Australian coastal management. *Ocean & Coastal Management*, *154*, 103–120. https://doi.org/10.1016/j.ocecoaman.2018.01.001

Toimil, A., Camus, P., Losada, I., Le Cozannet, G., Nicholls, R., Idier, D., & Maspataud, A. (2020). Climate change-driven coastal erosion modelling in temperate sandy beaches: Methods and uncertainty treatment. *Earth-Science Reviews*, *202*, 103110. https://doi.org/10.1016/j.earscirev.2020.103110

USGS. (2023). Current water data for Massachusetts under United States Geological Survey [Dataset]. USGS. Retrieved from https://waterdata.usgs.gov/ma/nwis/rt

Valiente, N. G., Masselink, G., Scott, T., Conley, D., & McCarroll, R. J. (2019). Role of waves and tides on depth of closure and potential for headland bypassing. *Marine Geology*, *407*, 60–75. https://doi.org/10.1016/j.margeo.2018.10.009

van Rijn, L. C. (1998). Principles of coastal morphology.

van Rijn, L. C. (2011). Coastal erosion and control. *Ocean & Coastal Management*, *54*(12), 867–887. https://doi.org/10.1016/j.ocecoaman.2011.05.004

Vieira da Silva, G., Toldo, E. E., Jr., Klein, A. H. D. F., & Short, A. D. (2018). The influence of wave-wind- and tide-forced currents on headland sand bypassing – Study case: Santa Catarina Island north shore, Brazil. *Geomorphology*, *312*, 1–11. https://doi.org/10.1016/j.geomorph.2018.03.026

Wishaw, D., Leon, J. X., Barnes, M., & Fairweather, H. (2020). Tropical cyclone impacts on headland protected bay. *Geosciences*, *10*(5), 190. https://doi.org/10.3390/geosciences10050190

Xie, D. (2023). Model setup for a reference scenario and the hydrodynamic data around Western Buzzards Bay (v3) [Dataset]. Zenodo. https://doi.org/10.5281/zenodo.10621597

Xie, D., Schwarz, C., Brückner, M. Z. M., Kleinhans, M. G., Urrego, D. H., Zhou, Z., & van Maanen, B. (2020). Mangrove diversity loss under sea-level rise triggered by bio-morphodynamic feedbacks and anthropogenic pressures. *Environmental Research Letters*, *15*(11), 114033. https://doi.org/10.1088/1748-9326/abc122

Xie, D., Schwarz, C., Kleinhans, M. G., Zhou, Z., & van Maanen, B. (2022). Implications of coastal conditions and sea-level rise on mangrove vulnerability: A bio-morphodynamic modeling study. *Journal of Geophysical Research: Earth Surface*, *127*(3), e2021JF006301. https://doi.org/10.1029/2021jf006301

References From the Supporting Information

Brakenhoff, L., Schrijvershof, R., van der Werf, J., Grasmeijer, B., Ruessink, G., & van der Vegt, M. (2020). From ripples to large-scale sand transport: The effects of bedform-related roughness on hydrodynamics and sediment transport patterns in Delft3D. *Journal of Marine Science and Engineering*, *8*(11), 892. https://doi.org/10.3390/jmse8110892

CIRES. (2014). *Cooperative Institute for Research in Environmental Sciences (CIRES) at the University of Colorado, Boulder. Continuously Updated Digital Elevation Model (CUDEM) - 1/9 arc-second resolution bathymetric-topographic tiles*. NOAA National Centers for Environmental Information.

Dean, R. G., & Dalrymple, R. A. (2004). *Coastal processes with engineering applications*. Cambridge University Press.

Marsooli, R., & Lin, N. (2018). Numerical modeling of historical storm tides and waves and their interactions along the US East and Gulf Coasts. *Journal of Geophysical Research: Oceans*, *123*(5), 3844–3874. https://doi.org/10.1029/2017jc013434

Warner, J. C., Geyer, W. R., & Lerczak, J. A. (2005). Numerical modeling of an estuary: A comprehensive skill assessment. *Journal of Geophysical Research*, *110*, C05001. https://doi.org/10.1029/2004jc002691

Willmott, C. J. (1981). On the validation of models. *Physical Geography*, *2*(2), 184–194. https://doi.org/10.1080/02723646.1981.10642213

Xie, D., Schwarz, C., Kleinhans, M. G., Bryan, K. R., Coco, G., Hunt, S., & van Maanen, B. (2023). Mangrove removal exacerbates estuarine infilling through landscape-scale bio-morphodynamic feedbacks. *Nature Communications*, *14*(1), 7310. https://doi.org/10.1038/s41467-023-42733-1

Zhu, Q., & Wiberg, P. L. (2022). The importance of storm surge for sediment delivery to microtidal marshes. *Journal of Geophysical Research: Earth Surface*, *127*(9), e2022JF006612. https://doi.org/10.1029/2022jf006612